Cureus Journal of Engineering

Open Access Original Article

Corrosion and Adhesion Performance of Ferric Ion-Based Hybrid Nano-Conversion Coatings on Aluminum Alloy

Received 06/17/2025
Review began 06/22/2025
Review ended 10/27/2025
Published 11/04/2025

DOI:
https://doi.org/10.7759/s44388-025-07832-3

Makanjuola Oki [1] , Ebitei Charles [2] , Peter P. Ikubanni [3]

1. Corrosion Science and Engineering, Wigwe University, Port-Harcourt, NGA 2. Corrosion Science and Engineering, Nigeria Civil Aviation Authority, Ikeja, NGA 3. Mechatronics Engineering/Advanced Engineering Materials, Bowen University, Iwo, NGA

Corresponding author: Peter P. Ikubanni, peter.ikubanni@bowen.edu.ng

Abstract

Efforts at partial or total replacement of environmentally unfriendly and carcinogenic chromate in conversion coatings on Al and its alloys are yielding some positive outcomes. This study investigated the corrosion and adhesion performance of novel conversion coatings on Al6061 alloy using an electrochemical test and microstructural examination of the alloy's surface. The results of the electrochemical assessments of ferric ions and hybrid coatings based on ferric ion/chromate as well as ferric ion/molybdate in 3.5% NaCl revealed the superiority of ferric coatings over hybrid coatings. Corrosion rate for ferric coatings was 0.037 mm/yr, while 0.246 mm/yr was recorded for ferric ions/chromate, and the rate for ferric ions/molybdate coatings was 0.304 mm/yr. From scanning electron microscopy, the coatings consisted of irregularly shaped materials that highlighted and decorated the grains and sub-grain boundaries of their substrates. However, cracked morphologies, which were thought to be weaknesses in the coatings, prevailed in hybrid coatings. Energy Dispersive X-ray analyzer, within the limits of detection, revealed that the elemental components of the coatings were Al and O for ferric coatings; Al, O, and Cr for Ferric/chromate; and ferric/molybdate had Al, O, and Mo, respectively. There were no obvious disparities in the adhesion performance of the coatings as revealed by pull-off adhesion tests after exposure to an atmospheric environment for 168 h. These pretreatments are suitable replacements for highly concentrated generic chromate conversion coatings due to lower costs for process effluent treatments compared to effluents from the latter.

Categories: Advanced Materials, Materials Engineering, Environmental Engineering and Sustainability
Keywords: sem/edx, hybrid conversion coatings, potentiodynamic polarization, adhesion, corrosion rate

Introduction

The combination of lightness, strength, and workability makes aluminum and its alloys ideal materials for mass-produced high-speed, light vehicles that are environment-friendly because of their low fuel consumption [1-3]. Efforts to make aluminum lighter and stronger have taken the central stage in research on the development of new composite materials based on nanoparticles and fibers of plants' origin [4-6]. These composite materials have proven to be lighter, stronger, and well-endowed with good mechanical properties. However, they are prone to localized corrosion, such as stress corrosion cracking and mesa-like pitting corrosion in highly acidic environments [7,8]. Thus, the strategy of weight reduction to reduce oil consumption by about 10% has resulted in a 6% reduction in environmental pollution caused by automobiles [9,10]. This environmental improvement inflicted various types of corrosion in Al because of the strengthening route employed to fit it into the strategic plan. Hence, corrosion prevention is essential for the preservation of the integrity and longevity of Al in engineering structures and equipment [11]. It is usual practice to apply a chromate conversion coating (CCC) on aluminum before painting, but chromate use has been limited by various protocols [12]. However, efforts are ongoing far and wide to replace chromates in conversion coating baths because of health and environmental considerations. A few of the "so-called" environmentally friendly substitutes, which are of low toxicity, have been suggested in the literature [13,14] and are acclaimed to outperform CCC.

Hybrid Mo-based CC, MoTiZr, was reported to be more resistant to corrosion in 3.5% NaCl than chromate, MoTi, and bare aluminum 6061 [15]. Ikubanni et al. [16] investigated aluminum alloy coated with hybrid chromate-phosphate conversion coatings. The conversion-coated samples were subjected to 100% relative humidity at 313 K for 480 h. These hybrid chromate-phosphate conversion-coated samples were compared with samples coated with chromate solution and uncoated aluminum alloy samples. The study revealed that the hybrid chromate-phosphate coatings improved the corrosion resistance and paint adhesion features of the Al alloy and compared favorably with the chromate coatings. The utilization of chromate-phosphate hybrid coating is relatively less environmentally toxic compared to chromate. Hence, the chromate-phosphate coatings were recommended as an alternative to chromate coating. In the quest to source alternative conversion coating solutions to the use of chromate coatings, the corrosion

How to cite this article
Oki M, Charles E, Ikubanni P P (November 04, 2025) Corrosion and Adhesion Performance of Ferric Ion-Based Hybrid Nano-Conversion Coatings on Aluminum Alloy. Cureus J Eng 2 : es44388-025-07832-3. DOI https://doi.org/10.7759/s44388-025-07832-3

inhibition performance of Al 6061 coated with hybridized *Hibiscus sabdariffa calyx* extract (HSCE) and vanadate salt was investigated. The obtained results were compared with Al 6061 samples coated with CCC. It was revealed that the relatively faster diffusion rate of the chelated Mo (VI) complex of the hybrid HSCE inhibited corrosion and provided a better barrier on the substrate [17].

Due to accelerated corrosion as a result of the inclusion of secondary reinforcement particles in aluminum matrix composites (AMCs), which presented the inclusions as cathodic sites, an investigation was carried out to mitigate this effect when the samples were subjected to aggressive corrosion environments. Ikubanni et al. [5] explored the application of potassium permanganate conversion coating (PPCC) solution on AMCs developed and compared the results with CCC samples. It was revealed that both the PPCC and CCC performed relatively well in inhibiting corrosion on the developed AMCs. The conversion coatings used on the substrate inhibited the delamination of the coating with the use of lacquer, hence, leading to reduced corrosion activities on the substrates. The environmentally friendly PPCC is adjudged to be a viable alternative to the carcinogenic CCC. In some other cases, the addition of poly-hydroxyl compounds to conversion coating solutions improved the performance of the resultant conversion coatings [12,17,18].

Furthermore, the use of Fe-based amorphous coating has proven to be corrosion and wear resistant. According to Ibrahim et al. [19], the reduced microstructural defects, such as grain boundaries in the amorphous structure of the coating, contributed to improved corrosion and wear resistance of engine parts. This conclusion revealed that amorphous metal coatings are versatile and promising solutions to increase the reliability of conversion coatings under various corrosive environments.

Thus, the current effort constitutes a first step in finding substitutes for chromate and improving the resistance of Al 6061, and later applying the engineered chemicals to hybrid Al composites of SiC and bio-based particles and/or fibers. These Al composites have posed considerable challenges in terms of reduction in their propensity for local corrosion phenomena [7,16]. These require attention to reduce the suitable conversion coatings procedure timeline, which translates to more efficient use of energy.

Materials And Methods

Materials

Al 6061 electrodes with a nominal composition (%) of 96.85 Al, 0.9 Mg, 0.7 Si, 0.6 Fe, 0.3 Cu, 0.25 Cr, 0.20 Zn, 0.10 Ti, 0.05 Mn, and 0.05 other elements were fabricated in the usual manner [7,16]. Conversion coating solutions were made up as follows: for ferric ions/chromate, ferric ions only, and ferric ions/molybdate, their corresponding salts, 4 g each, were dissolved in 1 L of water with some activators, and pH was adjusted with NaOH or HNO_3 to achieve a pH of 3.5 to 4. Laboratory-grade reagents and distilled water were employed throughout the experiment. For each hybrid coating solution, the precursor coating solutions were mixed in a ratio of 1:1. The electrodes were degreased and etched in a 10% NaOH solution, rinsed in water before de-smutting in 50% HNO_3, then washed again in a copious amount of water, and allowed to dry under the fan for 30 min. Distilled water and laboratory-grade reagents (BDH chemicals, UK) were used throughout.

Experimental procedures

Cleaned electrodes were treated in the various coating solutions for 3 min each, rinsed in water, and allowed to dry in air for 30 min. The coated electrodes were examined in a Scanning Electron Microscope, Model Pro X, equipped with an Energy Dispersive X-ray analyzer (EDX) running at high vacuum mode and 20 kV accelerating voltage. Further, coated electrodes were analyzed in 3.5% NaCl in a conventional three-electrode cell using a computer-controlled potentiostat/galvanostat (Autolab PGSTAT 302N). A platinum electrode, 1 cm^2, served as the counter electrode, Ag/AgCl (1 M KCl), as the reference electrode, and Al 6061 variously coated specimens were employed as working electrodes (WE). The area of the WE exposed to 3.5% NaCl was approximately 1 cm^2. Before each potentiodynamic polarization measurement, the electrode potential was allowed to stabilize while the open circuit potential (OCP) was recorded as a function of time for about 30 min. After this, a steady-state OCP corresponding to the corrosion potential (Ecorr) of the working electrode was obtained. The potential scans were executed automatically between 200 and -200 mV vs OCP at a rate of 10 mV/s. Fresh solutions were used after each potential sweep.

Other similarly treated electrodes were cross-hatched and exposed to the natural atmospheric environment for 168 hr. Beyond the exposure periods, the ASTM D3359-23 adhesion test procedure was applied to the specimens to assess the adhesion capabilities of the various conversion coatings. They were subsequently ranked 0B to 5B according to ASTM specification. The experimental procedure is displayed in Figure *1*.

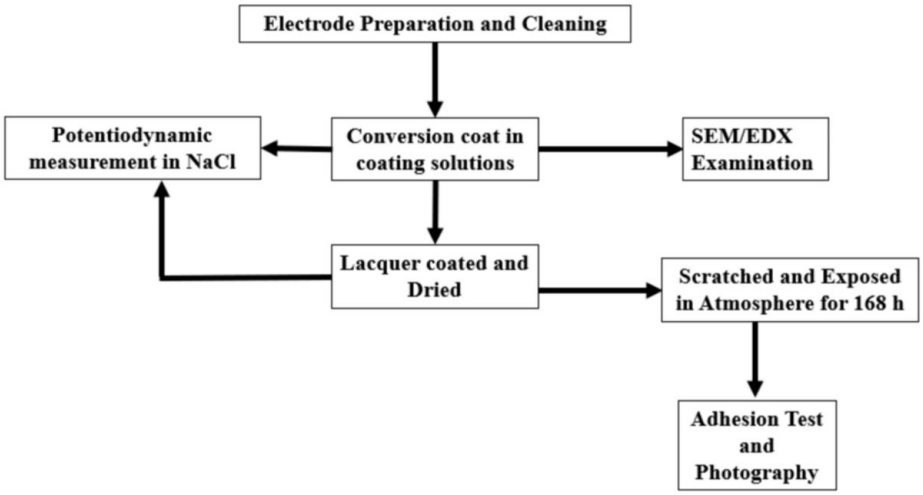

FIGURE 1: Schematic display of the experimental process

SEM, Scanning Electron Microscope; EDX, Energy Dispersive X-ray analyzer

Results And Discussion

Scanning Electron Microscopy and EDX examination

The scanning electron micrographs of the various conversion-coated specimens, as well as their EDX spectra, are displayed in Figure *2*, Figure *3* and Figure *4* and also in Table *1*, Table *2* and Table *3*, respectively. Figure *2* displays scalloped, continuous coating materials devoid of cracks, but it maps the grains and sub-grain boundaries of the substrate. The uneven surfaces, aided by irregularly shaped, thicker, light, and small-sized coating materials with a population density of about $7 \times 10^{10}/m^2$, are likely good anchor sites for subsequently applied organic coatings, thus giving rise to the mechanical keying of paint moieties to the substrates. Although chemical bonds among the chemical species on both sides are thought to play some part in improved paint adhesion, within the detection limits of the EDX attachment in the SEM, Fe was not detected in the coating material, as displayed in Table *1*. This indicates the low atomic % of Fe in the coating despite having a light brownish coloration after treatment of Al 6061 in the coating solution for 180 s. The light brown coloration indicated the presence of Fe ions in one manner or the another in the coating, albeit in a very low concentration below the detection of the EDS.

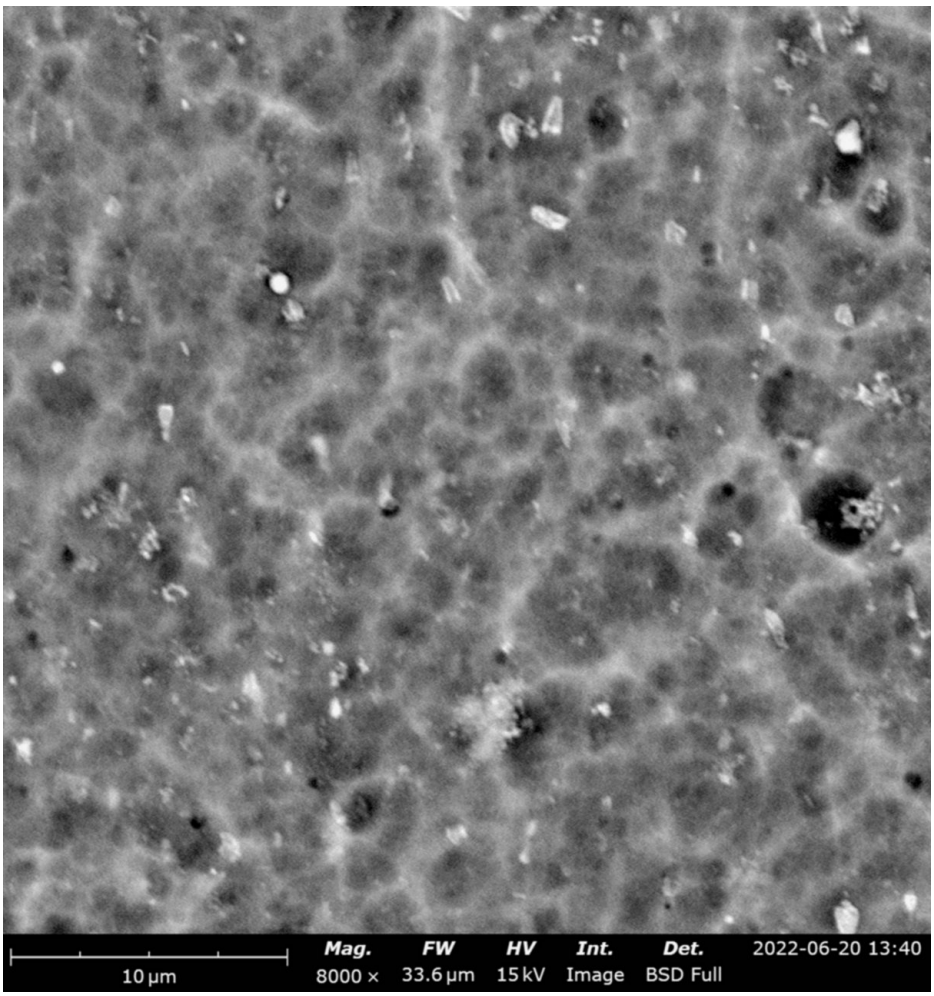

FIGURE 2: Scanning Electron Micrograph of Al 6061 treated in a ferric iron conversion coating solution for 3 min

Element Number	Element Symbol	Element Name	Atomic Conc.	Weight Conc.
13	Al	Aluminium	83.33	89.39
8	O	Oxygen	16.67	10.61

TABLE 1: EDX atomic composition of the coating developed on Al 6061 from ferric ions conversion coating solution for 3 min

EDX, Energy Dispersive X-ray analyzer

However, Al and O coating materials detected may be tainted with hydrated ferric/ferrous oxides and/or hydroxides. It is generally held that conversion coating formation on aluminum and other valve metals usually proceeds through the dissolution of substrates and precipitation of coating materials mechanism [16-18,20,21]. The thin oxide film on Al was initially removed by fluoride/activating agents in the coating solution thus releasing electrons from Al which are subsequently taken up by oxidants in the coating solution. In this case, ferric ions and dissolved oxygen are thus reduced to ferrous and hydroxide ions which are deposited as hydrated oxides and/or hydroxides when their equilibrium constants are achieved at the appropriate interfacial pHs.

The morphology of the coating developed on Al 6061 in a ferric/molybdate conversion coating solution for 3 min is displayed in Figure *3*. It can be observed that the coating developed as a massively cracked coating material because of the stress developed during the drying out of the initial gel-like coating

material which developed initially along the grains of the substrate. A school of thought [22] has it that the cracks act as anchoring sites for subsequently applied organic paints, thus improving the adhesion strength to the substrate, whereas others [23] believe that various bonds formed between moieties of organic coatings and compounds/atoms of conversion coatings combined may be responsible for the improvement in adhesion strength observed. To all intents and purposes, the EDX of the hybrid ferric/molybdate conversion coating materials (Table 2) revealed that it is composed of Al, O, and Mo compounds, probably hydrated.

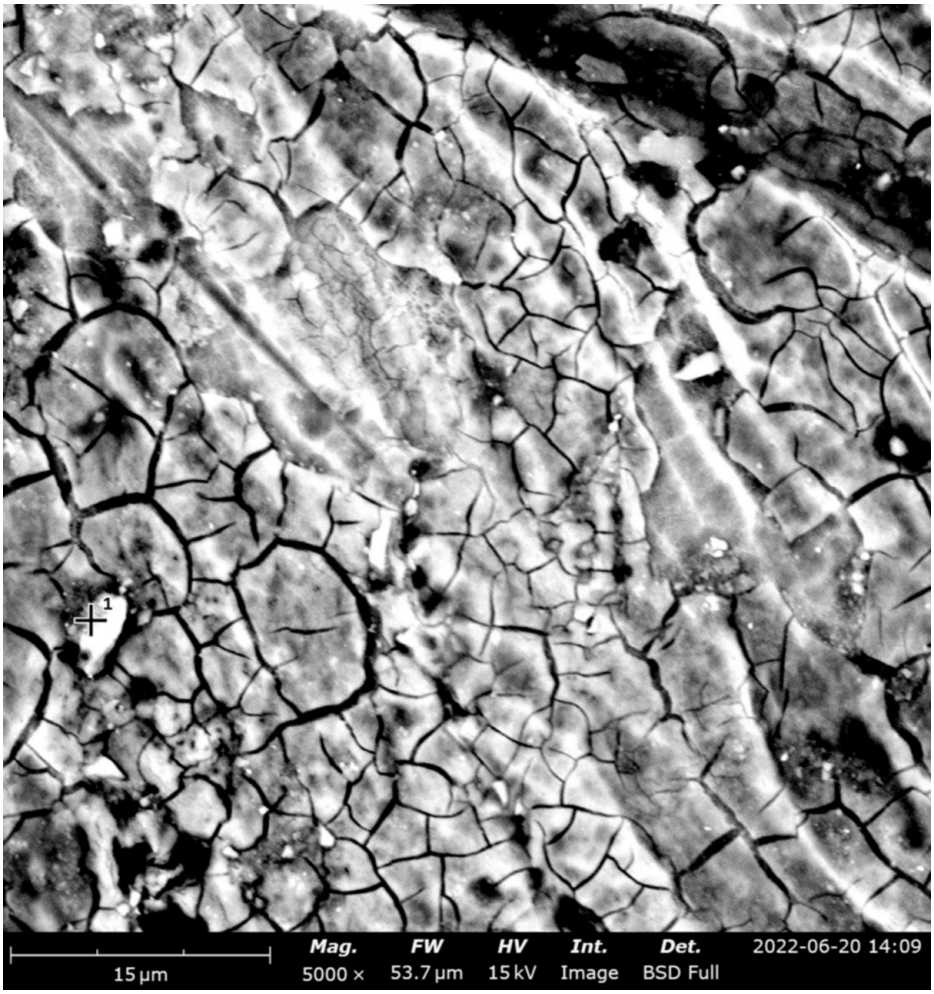

FIGURE 3: Scanning Electron Micrograph of Al 6061 treated in ferric ions/molybdate conversion coating solution for 3 min

Element Number	Element Symbol	Element Name	Atomic Conc.	Weight Conc.
13	Al	Aluminium	56.48	56.93
8	O	Oxygen	37.81	22.60
42	Mo	Molybdenum	5.71	20.47

TABLE 2: The EDX atomic composition of coating developed on Al 6061 from ferric ions/molybdate conversion coating solution for 3 min

EDX, Energy Dispersive X-ray analyzer

The conversion coating formed on Al 6061, from ferric/chromate conversion coating solution, Figure 4, displays a duplex coating system with islands of relatively thicker coating materials of chromate

compounds on a scalloped coating like those formed over the specimen coated in ferric ions conversion coating solution, Figure 2.

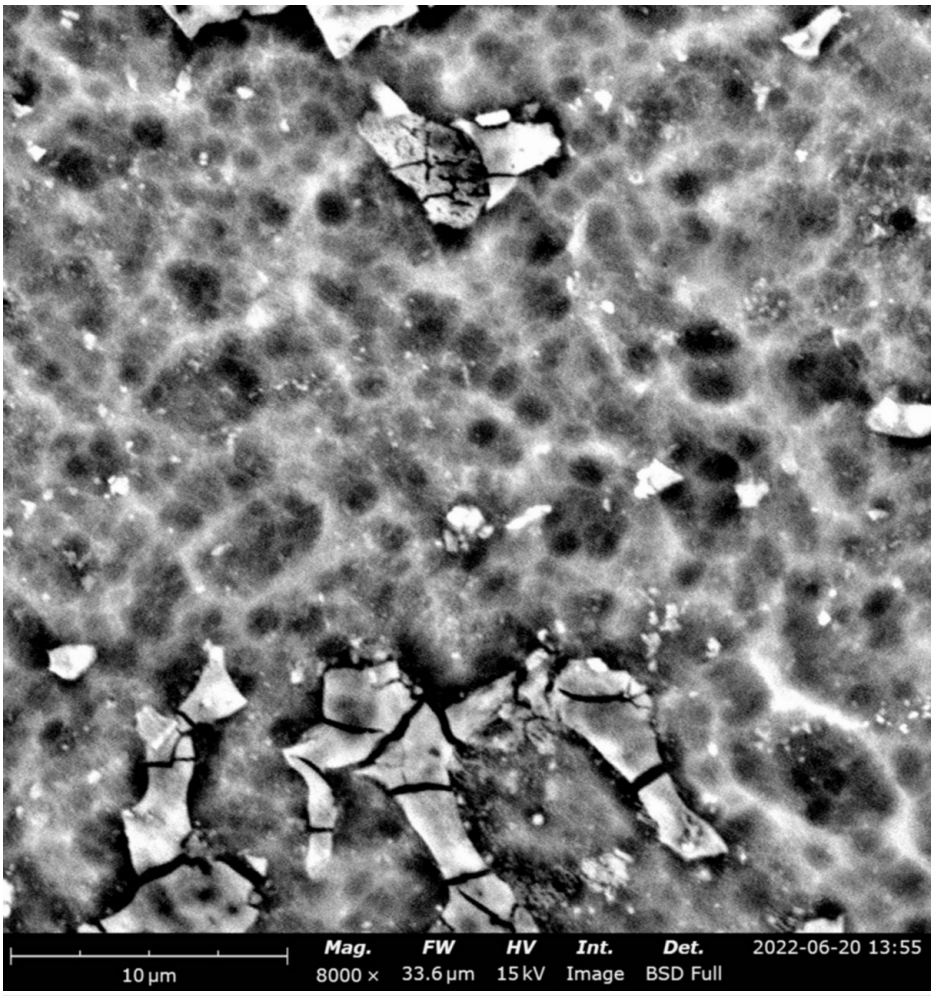

FIGURE 4: Scanning Electron Micrograph of conversion coating developed from ferric/chromate conversion coating solution for 3 min

The coating is composed of Al, O, and Cr compounds (Table 3). The cracked coating materials developed faster at inclusions, which are known to be cathode sites with respect to the general anodic areas of the substrate. However, EDX analyses at such regions only revealed Al, Cr, and O (Table 3) as the components of the coating. The inclusions must have been undermined during the anodic reactions at the periphery of the inclusions and could have fallen off into the coating solution. Other components, such as Fe, may have been present in quantities below the detection limit of the spectroscope. Additionally, the utilization of Fe-based amorphous coatings has been ascertained for its resistance to corrosion and wear. Microstructural defect reduction, including grain boundaries in the coating's amorphous structure, greatly enhances the corrosion inhibition of the substrate. This corroborates the findings of Ibrahim et al. [19] that amorphous metal coatings are versatile and are promising solutions to improve the reliability of conversion coatings under various corrosive environments.

Element Number	Element Symbol	Element Name	Atomic Conc.	Weight Conc.
13	Al	Aluminium	60.55	68.28
8	O	Oxygen	36.69	24.53
24	Cr	Chromium	2.53	5.51

TABLE 3: The EDX atomic composition of coating developed on Al 6061 from ferric/chromate conversion coating solution for 3 min

EDX, Energy Dispersive X-ray analyzer

Potentiodynamic polarization measurements in 3.5% NaCl solution

The potentiodynamic polarization curves obtained for the variously treated specimens examined in 3.5% NaCl solution are displayed in Figure *5*, and the corrosion properties of the specimens are in Table *4*, respectively. The shapes of the curves are similar; however, the pitting passivation potentials for the specimens differ greatly and range from about -0.51 V for specimens coated with hybrid ferric/molybdate/top lacquer coating and ferric/chromate to -0.71 V for Al 6061 specimens coated with ferric ions conversion coatings. The redox potential for Fe^{3+}/Fe^{2+} is 0.77 V, which may suggest that Fe^{3+} is involved in the pitting re-passivation reactions that occurred on the specimen in a saline environment. All the specimens, except for the specimens coated with ferric/molybdate/lacquer and specimens with only ferric/molybdate without a top coating of lacquer, displayed active pitting/re-passivation with their potentials constantly surging in opposite directions. These are expected with Al in saline environments as flawed coating regions on the substrate are constantly attacked by chloride ions. Such freshly breached areas are instantly healed by the by-products of reducible ions in the environment. These observations during pitting corrosion are often referred to as crack and heal events [24-26].

From Table *4*, it can be observed that the specimens with top coatings of lacquer are superior in terms of corrosion resistance to their counterparts without lacquer, except for the specimen conversion coated with ferric ions conversion coating solution. Curiously, the corrosion rate of the specimen without a top coating of lacquer was about three times more resistant than the lacquer-coated specimen, with a value of 0.037 mm/yr as against 0.099 mm/yr for the lacquer-coated specimen. Consequently, the corrosion potential, a measure of the propensity for corrosion to occur, was more negative at -0.711 V for the lacquered specimen than for the bare sample at -0.702 V. The aggressive environment may have penetrated through imperfections/flaws in the lacquer to initiate intensive corrosion reactions at such regions on the substrate under the lacquer.

The time frames for the separate potentiodynamic measurements were within 1 hr each; thus, it is believed that the loosely held ferric ions were readily available to stifle corrosion reactions on the substrate, whereas such ions were bound by the topcoat of lacquer and could not readily participate in corrosion reactions in the instance of the latter. The corrosion current densities for specimens without top coatings of lacquer are 3.2×10^{-6} A/cm^2 for ferric ions CC, 2.8×10^{-5} A/cm^2 for ferric/molybdate CC, and 2.12×10^{-5} A/cm^2 for ferric/chromate. These rates showed the superiority of bare ferric ions conversion coating over its hybrid counterparts with molybdate and chromate. In a similar experiment [17, 27], the corrosion rate of bare chromate CC in 3.5% NaCl solution was 1.6×10^{-6} A/cm^2; however, the lacquer-coated ferric CC at 1.3×10^{-6} A/cm^2 closely matched the corrosion rate of bare chromate CC. Table *4* describes the corrosion parameters obtained by Tafel extrapolations from the potentiodynamic curves displayed in Figure *5*.

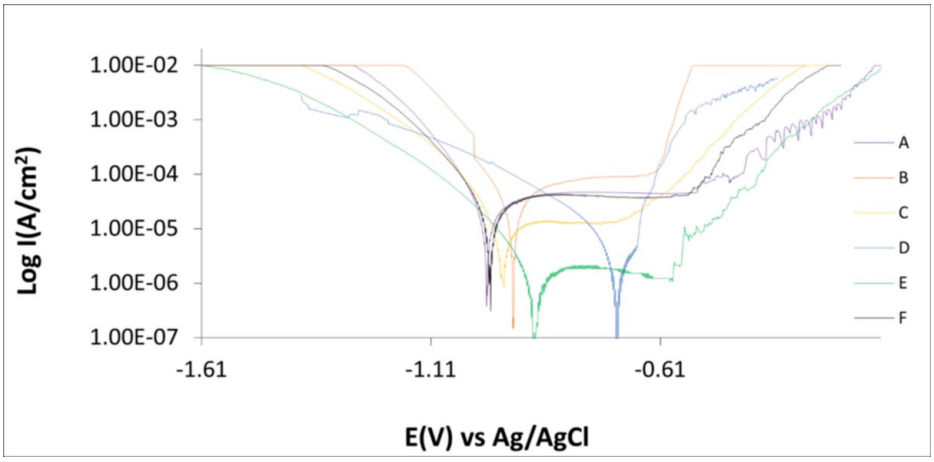

FIGURE 5: Potentiodynamic polarization curves for the various conversion-coated Al 6061 examined in 3.5% NaCl solution

A - Sample coated with ferric ions/ammonium molybdate conversion coating solution/lacquer.

B - Sample coated with ferric ions/ammonium molybdate conversion coating solution.

C - Sample coated with ferric ions conversion coating solution/lacquer.

D - Sample coated with ferric ions conversion coating solution.

E - Sample coated with chromate/ferric ions conversion coating solution/lacquer.

F - Sample coated with chromate/ferric ions conversion coating solution.

Sample	Corrosion Rate (mm/y)	Corrosion Current (A)	Corrosion Current Density (A/cm^2)	Corrosion Potential (V)	Polarization Resistance, Rp (Ω)	Cathodic Tafel Slope, Bc (V/dec)	Anodic Tafel Slope, Ba (V/dec)
A	0.259	2.41E-05	2.41E-05	-0.989	1068	12.15	2.749
B	0.304	2.85E-05	2.85E-05	-0.93	907.3	-18.87	3.08
C	0.099	9.43E-06	9.43E-06	-0.711	2724	0.17	12.95
D	0.037	3.21E-06	3.21E-06	-0.702	8016	-7.713	21.22
E	0.015	1.30E-06	1.30E-06	-0.881	19750	-10.58	0.89
F	0.246	2.12E-05	2.12E-05	-0.98	1212	-10.52	2.795

TABLE 4: Corrosion parameters obtained from potentiodynamic curves for the variously treated Al 6061 specimens in 3.5% NaCl solution

Paint adhesion performance

The cross-hatched specimens were exposed at a right angle to the ground, supported by Perspex in the natural atmosphere for 168 h, after which adhesion tests were applied separately on the specimens. To the naked eye, paint delamination was not observed on the specimens; thus, the specimens are ranked 5B according to the ASTM standard employed. However, the specimens coated in ferric/molybdate CC solution faded in color to a lighter shade of brown from their initial dark brown coloration. This change in the coloration denotes the formation and development of coatings on the substrates as revealed by Ikubanni et al. [5]. Apparently, the molybdate ions incorporated in the coating were leached from the specimen, probably to perform healing of corrosion processes on the surface of the specimen [28-30]. Apart from chemical interactions among components of the paint and conversion coatings, it is opined that mechanical interlocking provided by the roughness on micro and macroscopic scales, which are in abundance on the conversion coatings, aided improved adhesion bond to the substrates. Hence, the conversion coatings inhibited paint delamination and corrosion on the aluminium substrate in the

subjected environment. This confirms the barrier function of the conversion coatings for the substrate's protection when they are applied [5,16].

From the photographs displayed in Figure *6a*, the untreated specimen, which received the usual etching in NaOH followed by rinsing in 50% HNO_3 and a final rinse with a copious amount of water, showed myriad incipient pitting corrosions under a carpet of lacquer. Moisture that contaminated or otherwise migrated through holidays in the coating caused such damage during the exposure period. On the other hand, the conversion-coated specimens (b), (c), and (d) exhibited resistance to pitting corrosion. Thus, composite coatings of the three conversion coatings/lacquers employed in this investigation improved the pitting corrosion resistance of Al 6061 during natural atmospheric exposure. This corroborates the findings of Ikubanni et al. [5], which showed that the conversion-coated samples revealed improved pitting corrosion resistance.

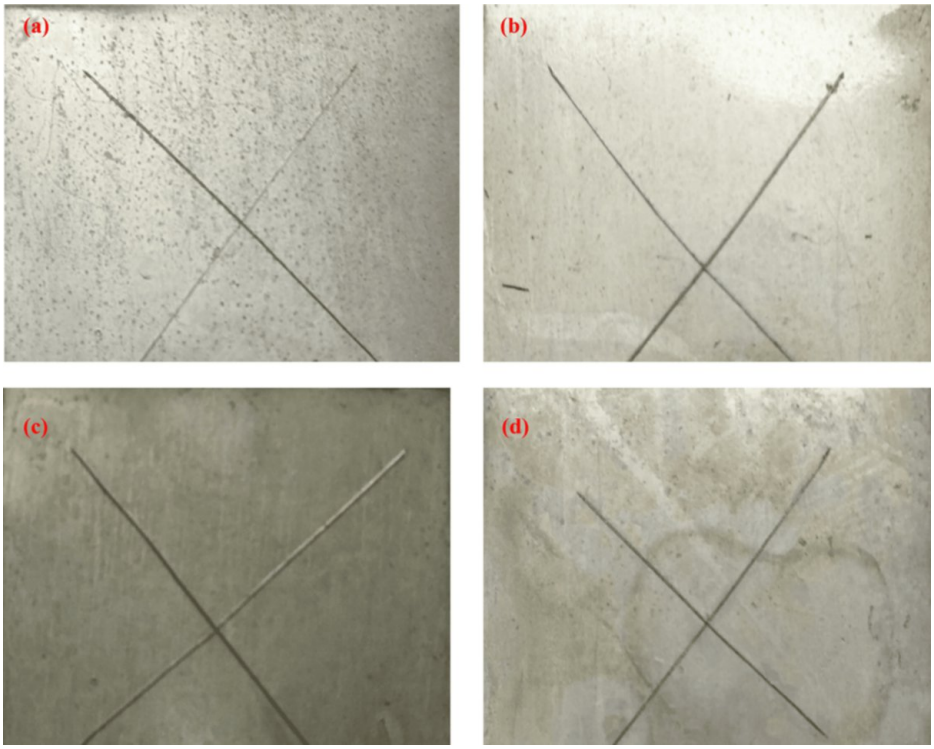

FIGURE 6: Conversion-coated Al 6061 with top coating of lacquer exposed to the natural atmosphere for 168 h before adhesion tests (a) untreated, (b) ferric ions CC, (c) ferric ions/chromate CC, and (d) ferric ions/molybdate CC

Conclusions

With further investigations, ferric ions conversion coating on Al 6061 may be a welcome alternative to CCC. However, the addition of either molybdate or chromate did not improve its corrosion performance, but adjustment of some coating parameters and factors could yield positive outcomes. The corrosion rates of the bare conversion coatings in 3.5% NaCl, as obtained from PDP measurements, are in the order of 0.037 > 0.246 > 0.304 (mm/yr) for ferric ions > ferric/chromate > ferric/molybdate conversion-coated specimens, respectively. The three conversion coatings resisted pitting corrosion and paint delamination on Al 6061. This shows the potency of the developed conversion-coated solutions. These conversion coating pretreatment solutions are suitable alternatives for highly concentrated generic and carcinogenic chromate conversion coatings in the view of their lower costs for process effluent treatments compared to effluents from the latter. These can be further employed for metal alloy pretreatments in various industries.

Additional Information

Author Contributions

All authors have reviewed the final version to be published and agreed to be accountable for all aspects of the work.

Acquisition, analysis, or interpretation of data: Peter P. Ikubanni, Makanjuola Oki, Ebitei Charles

Critical review of the manuscript for important intellectual content: Peter P. Ikubanni, Makanjuola Oki, Ebitei Charles

Concept and design: Makanjuola Oki

Drafting of the manuscript: Makanjuola Oki

Supervision: Makanjuola Oki

Disclosures

Human subjects: All authors have confirmed that this study did not involve human participants or tissue. **Animal subjects:** All authors have confirmed that this study did not involve animal subjects or tissue. **Conflicts of interest:** In compliance with the ICMJE uniform disclosure form, all authors declare the following: **Payment/services info:** All authors have declared that no financial support was received from any organization for the submitted work. **Financial relationships:** All authors have declared that they have no financial relationships at present or within the previous three years with any organizations that might have an interest in the submitted work. **Other relationships:** All authors have declared that there are no other relationships or activities that could appear to have influenced the submitted work.

References

1. Kumar J, Singh D, Kalsi NS, et al.: Comparative study on the mechanical, tribological, morphological and structural properties of vortex casting processed, Al-SiC-Cr hybrid metal matrix composites for high strength wear-resistant applications: Fabrication and characterizations. Journal of Materials Research and Technology. 2020, 9:13607-3615. 10.1016/j.jmrt.2020.10.001
2. Wang H, Ou X, Zhang X: Mode, technology, energy consumption, and resulting CO2 emissions in China's transport sector up to 2050. Energy Policy. 2017, 109:719-33. 10.1016/j.enpol.2017.07.010
3. Hosseinzadeh F, Rastegar S, Ashengroph M: Bioleaching of rare earth elements from spent automobile catalyst as pretreatment method to improve Pt and Pd recovery: Process optimization and kinetic study. Process Biochemistry. 2021, 105:1-7. 10.1016/j.procbio.2021.03.022
4. Ikubanni P, Oki M, Adeleke A, Adesina OS, Omoniyi PO, Akinlabi ET: Electrochemical studies of the corrosion behavior of Al/SiC/PKSA hybrid composites in 3.5% NaCl solution. Journal of Composites Science. 2022, 6:286. 10.3390/jcs6100286
5. Ikubanni PP, Oki M, Adeleke AA, et al.: Application of conversion coatings on aluminum matrix composites for corrosion protection. Portugaliae Electrochimica Acta. 2025, 43:165-76. 10.4152/pea.2025430302
6. Alaneme KK, Ekperusi JO, Oke SR: Corrosion behaviour of thermal cycled aluminium hybrid composites reinforced with rice husk ash and silicon carbide. Journal of King Saud University - Engineering Sciences. 2018, 30:391-97. 10.1016/j.jksues.2016.08.001
7. Aigbodion VS, Ezema IC: Multifunctional A356 alloy/ PKSAnp composites: Microstructure and mechanical properties. Defence Technology. 2020, 16:731-36. 10.1016/j.dt.2019.05.017
8. Ikubanni PP, Oki M, Adeleke AA, Onaolapo AS, Paramasivam P: Electrochemical investigation of the corrosion susceptibility of hybrid reinforced Al6063 with SiC and PKSA in 1.0 M sulfuric acid environment. Engineering Reports. 2024, 6:e12733. 10.1002/eng2.12733
9. Wu Y, Zhang S, Hao J, et al.: On-road vehicle emissions and their control in China: A review and outlook. Science of the Total Environment. 2017, 574:332-49. 10.1016/j.scitotenv.2016.09.040
10. Zhou J, Wang F, Wan X: Optimal design and experimental investigations of aluminium sheet for lightweight of car hood. Materials Today: Proceedings. 2015, 2:5029-36. 10.1016/j.matpr.2015.10.093
11. Nayak D, Rao SA, Gaonkar SL, Kumari PP: Hybrid metal matrix composite: a comprehensive review on its fabrication, corrosion behaviour and inhibition. Discover Applied Sciences. 2025, 7:791. 10.1007/s42452-025-07288-4
12. Zhu H, Li J: Advancements in corrosion protection for aerospace aluminum alloys through surface treatment. International Journal of Electrochemical Science. 2024, 19:100487. 10.1016/j.ijoes.2024.100487
13. Zhu W, Li W, Mu S, Fu N, Liao Z: Comparative study on Ti/Zr/V and chromate conversion treated aluminum alloys: Anti-corrosion performance and epoxy coating adhesion properties. Applied Surface Science. 2017, 405:157-68. 10.1016/j.apsusc.2017.02.046
14. Zhu W, Chen F, Luo Y, et al.: Vanadium and tannic acid-based composite conversion coating for 6063 aluminum alloy. Frontiers in Materials. 2021, 8:10.3389/fmats.2021.802468
15. Qian X, Huang F, Teng X, et al.: The preparation, corrosion resistance and formation mechanism of a new-type Mo-based composite conversion coating on 6061 aluminum alloy. Metals. 2023, 13:168. 10.3390/met13010168
16. Ikubanni PP, Oki M, Adediran AA, Akintola SA, Adeleke AA: Scanning and transmission electron microscopy examinations of composite hybrid chromate and chromate phosphate conversion coatings exposed in hot 100% relative humidity environments. Hybrid Advances. 2023, 3:100067. 10.1016/j.hybadv.2023.100067
17. Oki M, Ikubanni PP, Adediran AA, et al.: Electrochemical evaluation of corrosion control by composite hybrid vanadate conversion coatings on Al 6061. Portugaliae Electrochimica Acta. 2025, 43:309-22. 10.4152/pea.2025430504
18. Oki M, Charles E: Chromate conversion coating on Al-0.2wt.% Fe alloy. Materials Letters. 2009, 63:1990-991. 10.1016/j.matlet.2009.06.033
19. Ibrahim MZ, Zulkifli NWM, Syahmi AF, Sarhan AAD, Bakeer B: Wear and corrosion resistant iron-based amorphous coating in diluted biodiesel environment. Surface Innovations. 2025, 13:212-22. 10.1680/jsuin.24.00100

20. Shimizu K, Brown GM, Kobayashi K, Thompson GE, Wood GC: The role of electron tunnelling in the development of chemical conversion coatings on high purity aluminium. Corrosion Science. 1993, 34:1853-857. 10.1016/0010-938x(93)90022-9
21. Verdalet-Guardiola X, Fori B, Bonino J, Duluard S, Blanc C: Nucleation and growth mechanisms of trivalent chromium conversion coatings on 2024-T3 aluminium alloy. Corrosion Science. 2019, 155:109-20. 10.1016/j.corsci.2019.04.035
22. Kinloch AJ: Adhesion and Adhesive Science and Technology. Chapman and Hall, UK; 1987. 10.1007/978-94-015-7764-9
23. Thompson GE: Conversion Coatings. TALAT Lecture Series 5202. European Aluminium Association, 1994. 1-9.
24. Guan H, Buchheit RG: Corrosion protection of aluminum alloy 2024-T3 by vanadate conversion coatings. Corrosion. 2004, 60:284-96. 10.5006/1.3287733
25. Wang P, Dong X, Schaefer DW: Structure and water-barrier properties of vanadate-based corrosion inhibitor films. Corrosion Science. 2010, 52:943-49. 10.1016/j.corsci.2009.11.017
26. Oki M, Adediran AA, Ikechukwu A, Onokohwomo CO, Bosa C, Akintola SA, Adesina OS: Corrosion protection by novel conversion coatings on structural Al 6061. Applied Science and Engineering Progress. 2022, 16:10.14416/j.asep.2022.03.005
27. Oki M, Adediran AA, Ikubanni PP, et al.: Corrosion rates of green novel hybrid conversion coating on aluminium 6061. Results in Engineering. 2020, 7:100159. 10.1016/j.rineng.2020.100159
28. Peltier F, Thierry D: Review of Cr-free coatings for the corrosion protection of aluminum aerospace alloys. Coatings. 2022, 12:518. 10.3390/coatings12040518
29. Liang CS, Lv ZF, Zhu YL, Xu SA, Wang H: Protection of aluminium foil AA8021 by molybdate-based conversion coatings. Applied Surface Science. 2014, 288:497-502. 10.1016/j.apsusc.2013.10.060
30. Milošev I: Corrosion inhibition of aluminium alloys by molybdate ions: A critical review of the chemistry, mechanisms and applications. Corrosion Science. 2024, 229:111854. 10.1016/j.corsci.2024.111854